

Numerical experiments on the free motion of a point mass moving in a plane convex region: Stochastic transition and entropy

G. Benettin

Istituto di Fisica dell'Università and Gruppo Nazionale di Struttura della Materia, Padova, Italy

J.-M. Strelcyn

Département de Mathématiques, Centre Scientifique et Polytechnique, Université Paris-Nord, 93-Villetaneuse, France

(Received 25 May 1977)

We numerically investigate the behavior of a simple dynamical system, a plane billiard which by a continuous deformation of the border passes from a completely integrable system to a well-defined type of completely stochastic system, namely a K system. A stochastic transition is observed, with the usual coexistence of ordered and stochastic regions. Moreover, the stochastic region at certain intermediate stages appears to be separated into several invariant components. An estimate of the Kolmogorov entropy is presented.

I. INTRODUCTION

Since the celebrated paper by Fermi, Pasta, and Ulam in 1954,¹ a lot of numerical work has been done to investigate the ergodic properties of classical dynamical systems.²⁻⁵ By means of these numerical computations (or numerical experiments, as one often says), the new phenomenon of the stochastic transition has been observed.

This appears to be a rather general feature of those dynamical systems that are obtained by suitably perturbing integrable systems: for small enough perturbations the computations show only very regular orbits, lying apparently on invariant tori, while for larger perturbations a part of the tori seems to be destroyed, and erratic orbits instead appear, filling the so-called stochastic region. The change of behavior, as appears for example in the well-known Hénon-Heiles pictures,⁵ is rather impressive and certainly convincing, but presently very little understood by the theory, which cannot explain what happens when (and whether) invariant tori are destroyed.

In the present paper we are concerned with a billiard in a plane convex region, which by a suitable continuous deformation of the border passes from a disk to the so-called "stadion," that is, a region bordered by two equal parallel segments

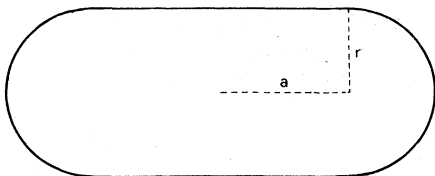


FIG. 1. The stadion.

and two half-circles (see Fig. 1). While the circular billiard is completely integrable,⁶ the billiard in the stadion, as proved by Bunimovich,⁸ is a K flow, i.e., certainly a flow with very strong stochastic properties. Since a K flow is ergodic, the disappearance of the invariant tori at the final stage is guaranteed. Moreover, the continuous passage from a completely integrable system to a K flow strongly suggests that during the intermediate stages a stochastic transition should take place, the features of which can be investigated by means of numerical experiments. Actually, we observed coexistence of invariant tori and a stochastic region,⁹ as in the other examples of stochastic transition. As a second feature, a separation of the stochastic region into invariant components has been observed when our billiard is sufficiently close to being completely integrable. Some mathematical results, reported in the Appendix, give a certain support to these numerical results.

To distinguish ordered and stochastic regions, and to characterize the invariant components of the latter, we employed two techniques: the graphical analysis of the mapping induced in a convenient section by the billiard flow, and the numerical computation of its maximal Lyapunov characteristic number. This latter technique has been employed in several papers^{3,4,11,12}; Ref. 12 contains in particular an analysis of its theoretical support. As shown in Ref. 12, these techniques, employed together, allow one to give an estimate of the Kolmogorov (or metric) entropy⁶ of systems of two degrees of freedom.

The outline of the present paper is as follows: Section II reports some preliminary computations concerning the extremal situations of the billiard in the disk and in the stadion. Section III contains

the description of the stochastic transition in its intermediate stages. Section IV contains the numerical estimate of the entropy; the method is improved with respect to that of Ref. 12. The Appendix contains some mathematical comments and remarks. This paper has been written as far as possible in a self-contained way, but a familiarity with Ref. 12 can be useful.

II. EXTREMAL SITUATIONS OF DISK AND STADION

A. Generalities

Let Q be a compact connected region of the plane R^2 , bounded by a differentiable border Γ . The dynamical system describing the free motion with unit velocity of a point mass in Q , with the law of elastic collisions at the border, is known as a billiard in Q . [For details and references, see Refs. 7, 13, 14, and 18.] In a natural way one identifies the billiard in Q with a flow $\{T^t\}$ on a three-dimensional manifold (with border) $M = Q \times S^1$, where S^1 denotes the unit circle, i.e., the set of all two-dimensional vectors of Euclidean length 1. The coordinates of a point $(q, v) \in M$ will be denoted by (q_1, q_2, θ) , where (q_1, q_2) are Cartesian coordinates of the point $q \in Q$ and θ is the angle between the velocity vector $v \in S^1$ and the q_1 axis. Let $|Q|$ denote the area of Q . The normalized measure $d\mu_L = (1/2\pi |Q|) dq_1 dq_2 d\theta$, which we shall call Liouville measure, is clearly invariant under the flow $\{T^t\}$; the ergodic properties of $\{T^t\}$ discussed in the present paper are referred only to this measure.¹⁵

As billiards are not differentiable Hamiltonian systems, the usual definition of completely integrable systems cannot be directly applied. However, the main property of the latter systems is that their phase space decomposes into the union of invariant tori, on which the motions are quasi-periodic (or periodic). It is easy to see geometrically that such a decomposition takes place in the case of the circular billiard, if one uses in its phase space the global system of coordinates (τ, η, s) which is defined in the beginning of Sec. IV, and if one considers the conservation of the angular momentum $L(q_1, q_2, \theta) = q_1 \sin \theta - q_2 \cos \theta$. One can then consider the billiard in the disk as a completely integrable system.

On the other hand, there exists a very particular class of plane convex regions, in which the billiards are K flows, as proved by L. A. Bunimovich.⁸ The simplest example is the so-called "stadium," which is a region whose border Γ is the union of two equal parallel segments of length $2a > 0$ and of two half circles of radius $r > 0$, as shown in Fig. 1. Γ has a continuous first derivative.

As a first computation, we can apply to the stadium and to the disk the already quoted technique for computing the maximal Lyapunov characteristic number (LCN). The definition of such numbers and the numerical technique are briefly recalled in Sec. IIB, while the results of the computations are presented in Sec. IIC.

B. The Lyapunov characteristic numbers

LCN's can be defined for a rather general class of flows or mappings; for simplicity we restrict ourselves to the case of a plane billiard in a region with differentiable border. In the exposition we follow the work by Oseledec.¹⁰

Denote by \tilde{M} the boundary of M , i.e., let $\tilde{M} = \{x = (q, v) \in M: q \in \Gamma\}$, and by E_x the tangent space to the manifold M at the point $x \in \tilde{M}$. For any t , apart from the denumerable set $\Omega(x) = \{t \geq 0: T^t x \in \tilde{M}\}$, the tangent application $dT_x^t: E_x \rightarrow E_{T^t x}$ is well defined, and the following statements can be proved.

For μ_L almost any $x \in M$, and for any nonzero tangent vector $e \in E_x$, the limit

$$\lim_{\substack{t \rightarrow \infty \\ t \notin \Omega(x)}} (1/t) \ln \|dT_x^t(e)\| = \lambda(x, e)$$

exists and is finite ($\|\cdot\|$ denotes here the Euclidean norm in the tangent space, induced by the Euclidean metric $dq_1^2 + dq_2^2 + d\theta^2$ in M). Moreover, $\lambda(x, e)$ depends on the direction of e , but not on its length and as e varies in E_x it can assume at most three different values, the Lyapunov characteristic numbers of the flow $\{T^t\}$ at the point x . Furthermore, for almost any $e \in E_x$, $\lambda(x, e)$ takes its maximal value $\lambda_{\max}(x)$, which turns out to be non-negative. It is clear that λ_{\max} is constant along the trajectories of the flow $\{T^t\}$.

Roughly speaking, λ_{\max} measures the mean rate of exponential divergence of the majority of trajectories surrounding the one passing through x .

The theory of the LCN's allows one to produce an unambiguous definition of stochasticity by saying that the stochastic region S coincides with all points $x \in M$ through which pass trajectories with $\lambda_{\max} > 0$. It could be easily seen that S is empty for the circular billiard. The stochastic region S is clearly flow invariant; if flow-invariant subsets of S exist, with the (empirical) properties of being of positive μ_L measure and not decomposable in the sum of smaller subsets of the same kind, we shall speak of stochastic components.⁴

The numerical technique for computing λ_{\max} is described in Ref. 12 for the slightly different case of a differentiable flow, and will be now shortly resumed and adapted to the present situation. The method is based on the approximate

identification of a sufficiently small vector $e \in E_x$ with a suitable segment \tilde{e} , of length $|\tilde{e}| = \|e\|$, with ends in x and in a close point $y \in M$. Denote by \tilde{e}_t the evolved segment, i.e., the segment with ends in $T^t x$ and $T^t y$; for all times t such that $|\tilde{e}_t|$ is sufficiently small, one has $|\tilde{e}_t| \approx \|dT_x^t(e)\|$. By a trick, which makes use of the linearity of dT_x^t , one can avoid the difficulty arising from the divergence of the trajectories, and carry on the computation for an arbitrarily long time. Namely, after a not too long time τ_1 , one replaces the segment \tilde{e}_τ by the segment $\tilde{e}_{\tau_1}^{(1)}$, having an end in $T_{x_1}^{\tau_1}$ and the same direction as \tilde{e}_{τ_1} , but with length $|\tilde{e}_{\tau_1}^{(1)}|$ equal to the original length $\|e\|$ (see Fig. 2). One can then write, for t not too much larger than τ_1 ,

$$|\tilde{e}_t^{(1)}| \approx \beta_1 \|dT_x^t(e)\|,$$

where β_1 is the reduction factor, i.e., $\beta_1 = \|e\| / |\tilde{e}_{\tau_1}|$. At arbitrary, not too large, time intervals $\tau_2, \dots, \tau_n, \dots$ the procedure is iterated, and thus one has

$$|\tilde{e}_t^{(n)}| \approx \beta_1 \times \beta_2 \times \dots \times \beta_n \|dT_x^t(e)\|,$$

for

$$t - \sum_{i=1}^n \tau_i \geq 0,$$

but not too large. At the moment t at which the n th iteration has been done, one computes the parameter

$$k_t(x, \tilde{e}) = -\frac{1}{t} \sum_{i=1}^n \ln \beta_i \approx \frac{1}{t} \ln \frac{\|dT_x^t(e)\|}{\|e\|}.$$

For almost any \tilde{e} , in particular, for a random choice of \tilde{e} , if $|\tilde{e}|$ is sufficiently small, one expects the following properties to be satisfied: (i) for any t , the length $|\tilde{e}|$ is irrelevant; (ii) for large t , the direction of \tilde{e} becomes irrelevant; (iii) for large t , $k_t(x, \tilde{e})$ approaches a well-defined limit value that one identifies with $\lambda_{\max}(x)$.

Let us now turn to our particular billiards, and see what follows from applying this technique.

C. λ_{\max} for the stadion and for the disk

Our numerical experiments have been performed on a CDC-CY76, with a precision of 14 digits. The

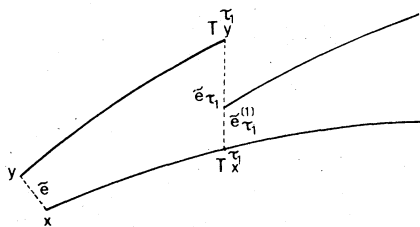


FIG. 2. Illustrating the procedure for computing λ_{\max} .

orbits have been followed by a simple geometrical algorithm, so that only round-off errors are present. For practical reasons, we found it convenient to perform the replacement of segments, as described in Sec. II B, immediately after a reflection; we have chosen the first reflection after a fixed time interval τ_0 . Typically it was $\tau_0 = 5$, and $|\tilde{e}| \approx 1.9 \times 10^{-7}$.

Since the billiard in the stadion is ergodic, the limit value $\lambda_{\max}(x)$ for this system is μ_L almost everywhere constant; and in agreement with the idea that a K flow has strong stochastic properties, it is natural to expect $\lambda_{\max}(x) > 0$. Actually, in Fig. 3, curves a and b show on a log-log scale the behavior of k_t as a function of t , for the stadion with $a = r = 1$, and two different initial points x . It appears clearly that a limit value has been approached, namely, $\lambda_{\max} \approx 0.43$. Several other initial data have been considered with the same result. Concerning properties (i) and (ii) given in Sec. II B, accurate checks have been made. For example, by choosing $|\tilde{e}|$ ten times larger, the corresponding change in k_t , at any t , is less than 10^{-5} ; by varying the direction of \tilde{e} , the change in k_t is almost 10^{-3} for $t = 10^2$, about 10^{-4} for $t = 10^3$, and less than 10^{-5} for $t \geq 10^4$. Also, the time interval τ_0 turns out to be largely irrelevant: for example, by doubling it, the corresponding change in k_t is less than 10^{-5} . This accuracy in the measurement of λ_{\max} is somehow higher than in analogous computations performed on other systems^{11,12}; to this probably contributes the relatively high accuracy by which one can follow billiard orbits.

Curve c of Fig. 3 shows the behavior of k_t for $a = 0$, i.e., for the disk. The difference with respect to curves a and b is evident; for curve c one has approximately $k_t = \text{const} \times t^{-1}$, so that one is allowed to take zero as the limit value. Similar checks of accuracy have been made also in this case with similar results.

While the billiard in the stadion ($a > 0$) is a K flow, the billiard in the disk ($a = 0$) is a completely integrable system, as already remarked. As a consequence, the transition from positive to vanishing a is in a sense abrupt; nevertheless, some continuity occurs. Indeed, for $a \ll r$ the billiard is found to be very little stochastic, i.e., λ_{\max} rapidly decreases towards zero as a tends to zero. More precisely, let $\gamma = a/r$, and denote the area of the corresponding stadion by

$$Q = Q(a, r) = 4ar + \pi r^2.$$

The Q dependence of λ_{\max} at fixed γ is trivial: Simple similarity considerations show that one has

$$\lambda_{\max}(\gamma, Q') = (Q/Q')^{1/2} \lambda_{\max}(\gamma, Q).$$

The γ dependence of λ_{\max} at fixed $Q = Q(1, 1)$ has

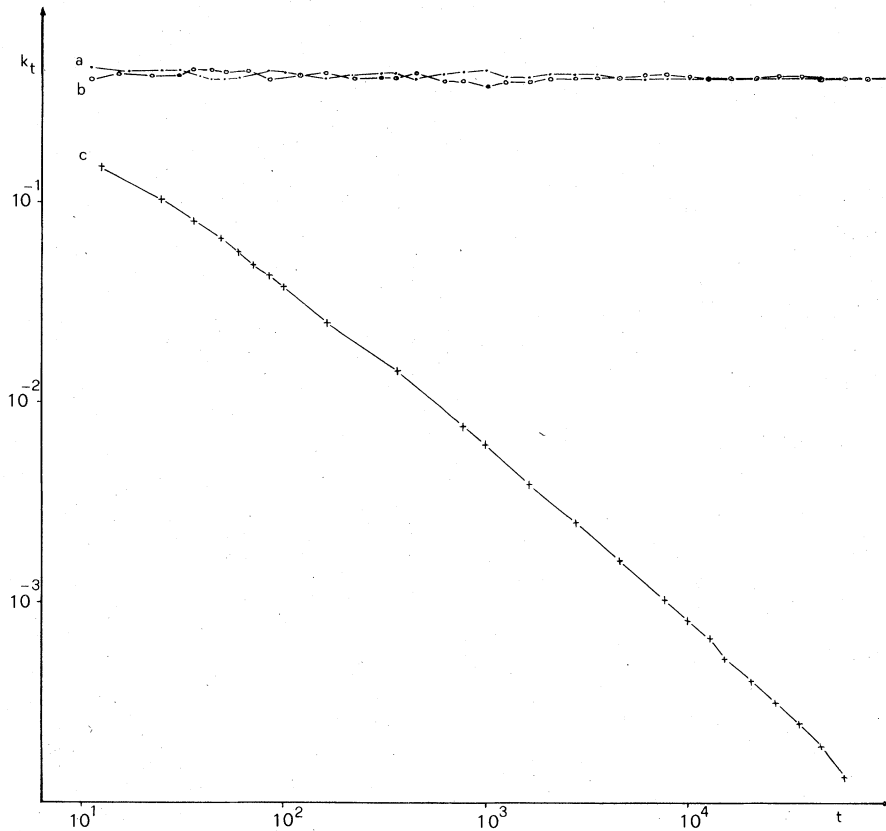


FIG. 3. Behavior of k_t in the case of the stadion (curves a and b) and of the disk (curve c).

been numerically investigated, and the resulting curve is reported in Fig. 4. One can observe the rapid decrease of λ_{\max} for $\gamma \rightarrow 0$, and a slower decrease for $\gamma \rightarrow \infty$, with a flat maximum near $\gamma = 1$. Vertical bars in Fig. 4 represent the uncertainty by which λ_{\max} has been determined: they correspond to the residual oscillation of k_t around its limit value.

As a final remark, the "stabilization time," i.e., the time required for k_t to reach its limit value, is larger when γ is very small. One can explain this feature by saying that, roughly speaking, the time required by an erratic trajectory to approximately fill M is very large when γ is very

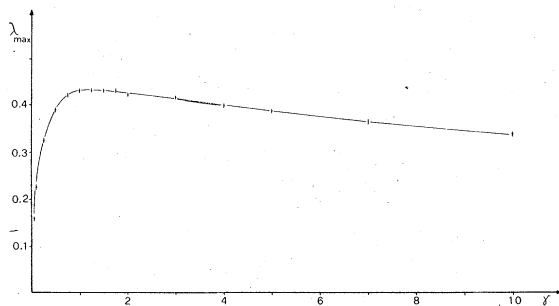


FIG. 4. Behavior of λ_{\max} as a function of γ .

small; presumably it tends to infinity when γ tends to zero. This is also one feature, by which continuity is exhibited.

III. THE GENERALIZED STADION

A. The global section

Consider the general case of a compact convex region Q , with differentiable border Γ . Let $q_0 \in \Gamma$, and denote by ψ the natural parametrization of Γ given by the length on Γ oriented counterclockwise, with origin in q_0 . Denoting by $|\Gamma|$ the length of Γ , one has clearly $0 \leq \psi < |\Gamma|$.

To any collision of the moving point with the border one can associate the coordinate ψ of the point of collision and a coordinate α , given by the oriented angle from the inner normal to Γ at the point of collision to the emerging velocity vector. Let N be the cylinder parametrized by the coordinates (ψ, α) with $0 \leq \psi < |\Gamma|$ and $|\alpha| \leq \frac{1}{2}\pi$, i.e., the set of all possible collisions. N can be naturally considered as a global section¹⁶ of the billiard flow; indeed, given a trajectory, to any collision with the boundary a new collision certainly follows. The flow $\{T^t\}$ on M induces then in a natural way a homeomorphism ϕ of the interior of N into itself, obtained by associating to each collision the next

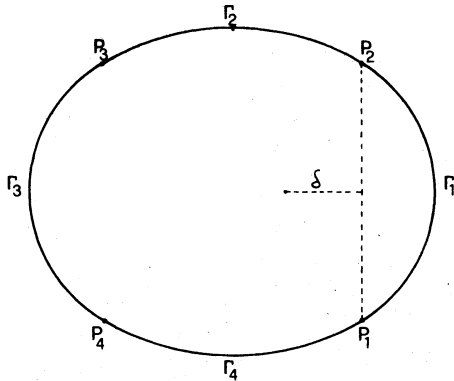


FIG. 5. The generalized stadium.

collision. If Q is strictly convex, one can extend the homeomorphism in a continuous way to the whole N , defining ϕ on the curves $\alpha = \pm \frac{1}{2}\pi$ as the identical mapping. One is then allowed to identify these curves, thus considering N as a two-dimensional torus, and ϕ as a homeomorphism of this torus. In general, if Γ is a curve of class C^k , $k \geq 2$, then ϕ is a diffeomorphism of class C^{k-1} of the torus N .

After these preliminary considerations, we pass

now to the description and the numerical study of the generalized stadium. For practical convenience, we shall use on N the slightly different coordinates (η, s) , with $\eta = \psi/|\Gamma|$ and $s = \sin\alpha$. As proven in Refs. 7 and 13 (see also Ref. 14), the normalized measure on N ,

$$d\nu_L = (1/2|\Gamma|) \cos\alpha d\psi d\alpha = \frac{1}{2}d\eta ds,$$

is ϕ invariant.

B. The generalized stadium

Consider four points P_1, \dots, P_4 at the vertices of a square of side-length two, and four arcs of circle $\Gamma_1, \dots, \Gamma_4$ disposed as in Fig. 5, with common tangent in P_1, \dots, P_4 , thus delimiting a symmetric convex oval-shaped region Q . Let δ be the distance from the center of Γ_1 to the side P_1-P_2 of the square; then one has the stadium for $\delta=0$, and a circle for $\delta=1$. One can call this region the generalized stadium.

At variance with the case of the preceding section, where for any value of $a > 0$ one had a K flow, the ergodic properties of a billiard in the generalized stadium for $0 < \delta < 1$ are not known theoretically. Numerical experiments indicate that the

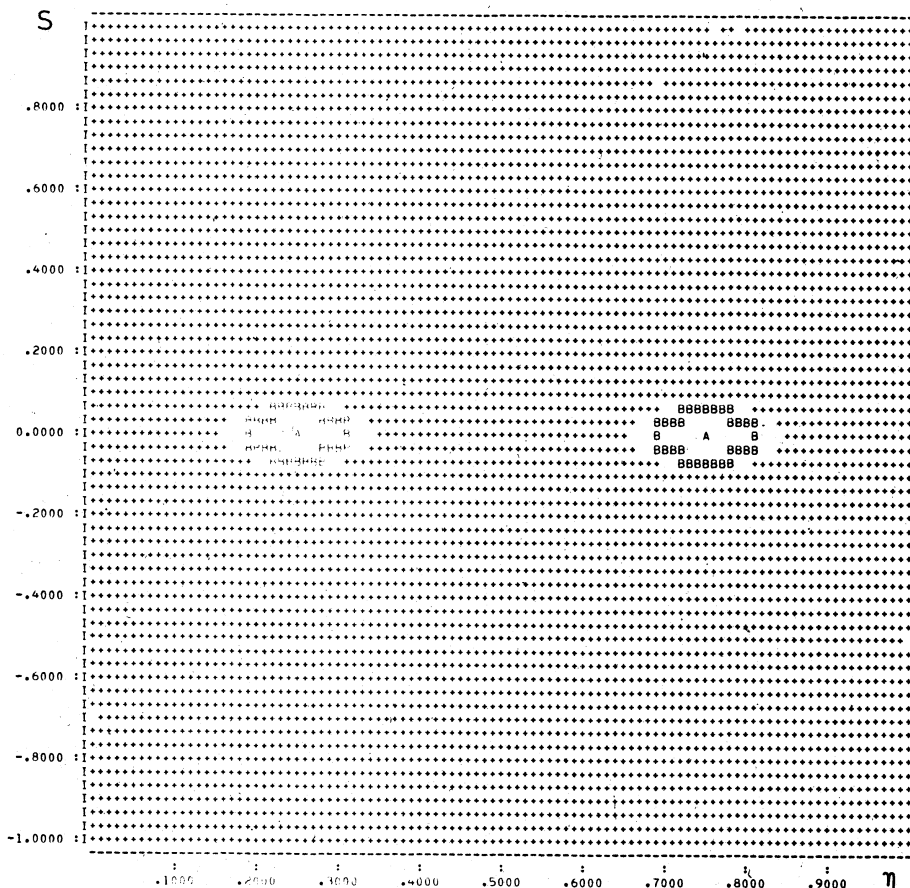


FIG. 6. Graphical analysis of ϕ for $\delta=0.01$.

continuous variation of δ from 1 to 0 induces in the system a stochastic transition, with coexistence of ordered and stochastic regions for any $\delta \neq 0, 1$.

Our basic tools have been the already explained technique for computing λ_{\max} , and a graphical study of the mapping $\phi: N \rightarrow N$, introduced in Sec. IIIA. We employed for N the coordinates (η, s) , choosing the origin q_0 of the coordinate η in the middle point of Γ_1 .

For each fixed value of δ , several initial data $x \in N$ have been considered, and the points $x, \phi x, \dots, \phi^n x, \dots$ have been marked on N . The different character of the trajectories is then easily visualized. A periodic orbit in M , undergoing k collisions before closing, gives rise to k isolated points in our figures; orbits of quasiperiodic type should instead appear as a set of points densely filling suitable closed curves. Concerning λ_{\max} , one expects to find numerically a vanishing value in any region where quasiperiodic orbits prevail. Finally, a stochastic orbit should appear as a set of points filling densely a certain area, and correspondingly λ_{\max} can be expected to be positive.

This actually occurs, and coexistence of different kinds of trajectories has been observed for any $\delta \neq 0, 1$. Figure 6 refers to $\delta = 10^{-2}$, and shows

a large stochastic "sea," filled by a single orbit (symbol +), with a couple of small "islands" in which one finds quasiperiodic orbits (e.g., symbol B) around a closed orbit (symbol A). By increasing δ , many other islands become evident. For example, Fig. 7 shows for $\delta = 0.6$ a quite complicated structure: within the stochastic sea, filled by a single trajectory, one can see many islands apparently surrounding closed orbits. At least for the simpler among these, it is possible to compute the coordinates of their traces in N , by means of elementary geometrical considerations (see Fig. 8). They correspond with high accuracy to the centers of the islands, as appearing for example in Fig. 7. One can notice, within the sea, several "white holes": they correspond to other more complicated chains of islands, and one is led to suppose that islands of any size exist, being eventually dense in the sea, as conjectured in Refs. 4 and 5 in a similar setting. Figure 9, which is an enlargement of a detail of Fig. 7, seems to confirm this conjecture.

Concerning λ_{\max} , we found as expected a vanishing value in the islands, and a positive value in the sea. Moreover, up to $\delta = 0.75$, we found just one stochastic component: a single orbit fills it, and λ_{\max} is constant within it. Considered as a function of

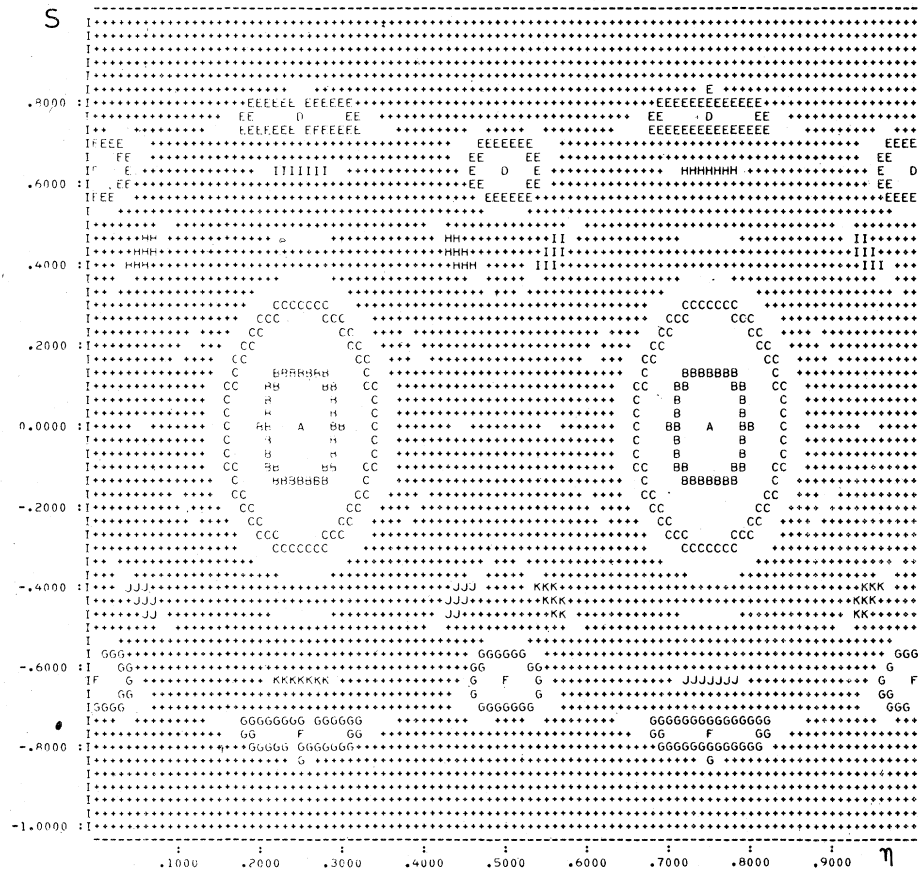


FIG. 7. Graphical analysis of ϕ for $\delta = 0.6$.

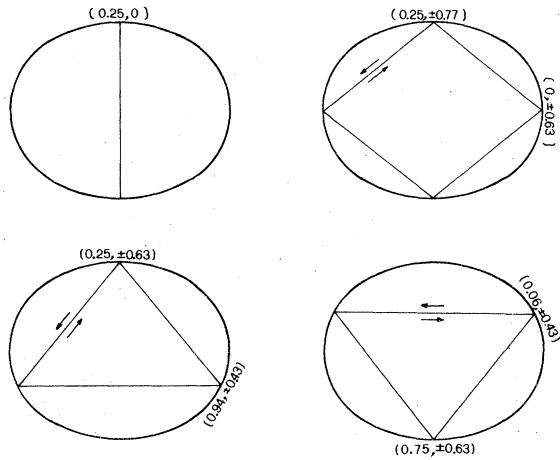


FIG. 8. Illustrating the more simple periodic orbits. The coordinates of the collisions, relative to $\delta=0.6$, are indicated.

δ , λ_{\max} decreases when δ passes from 0 to 0.6, and seems to be constant between 0.6 and 0.75. In the latter interval, numerical computations are particularly hard: the stabilization time increases very much, and a typical orbit requires a very long

time for invading the sea. To these facts a substantial change in the properties of our system is associated. Indeed, for $\delta \geq 0.76$, one finds that the sea has been subdivided into more than one stochastic component: A trajectory starting in one of them fills it, but never goes out, and correspondingly λ_{\max} is constant within each component, but assumes, in general, different values in the different components.

Figure 10 shows the separation of the sea into stochastic components when it firstly occurs, i.e., for $\delta=0.76$. Figure 11 shows the situation for $\delta=0.85$ (because of the symmetry of the whole picture, only a quarter has been reproduced). Correspondingly, Fig. 12 shows the curves $\ln k_t$ vs $\ln t$ for $\delta=0.85$ and initial points chosen in three different components. Different limits are clearly approached. By increasing δ , the number of stochastic components increases rapidly: 11 for $\delta=0.85$, and at least 13 for $\delta=0.9$, so that N appears to be divided into thin strips. In the limit $\delta=1$, as s is an integral of motion, N is covered by an infinite set of invariant lines, and once again continuity is exhibited.

When, by increasing δ , a stochastic component

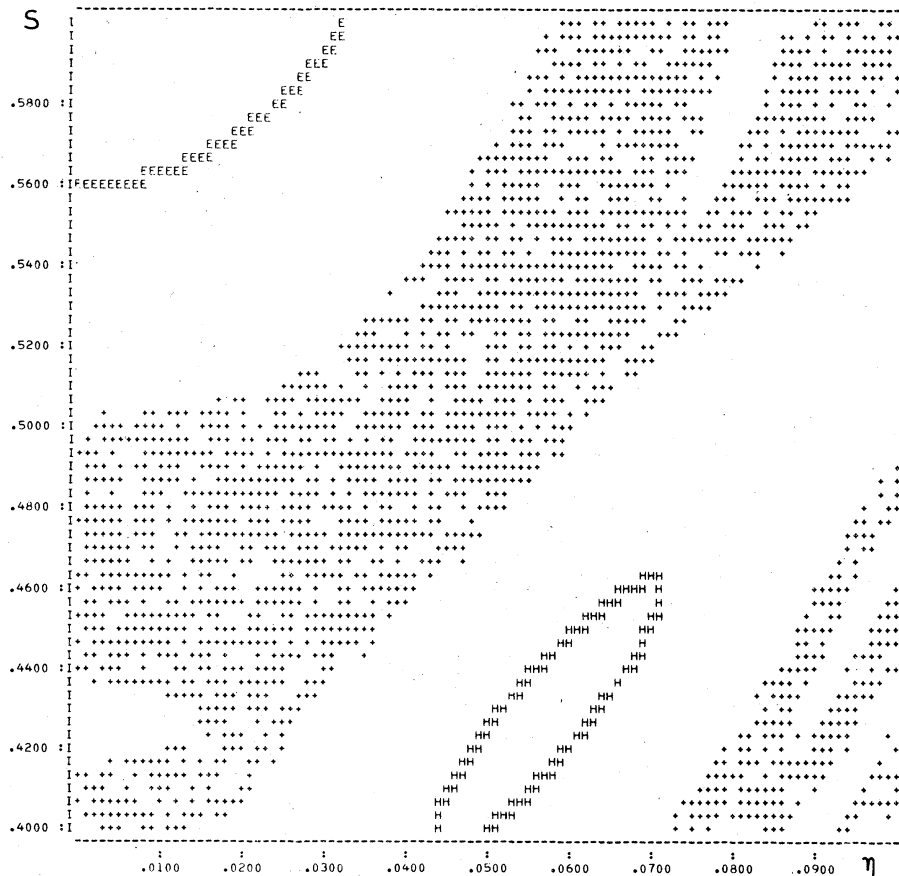


FIG. 9. Enlargement of a detail of Fig. 7.

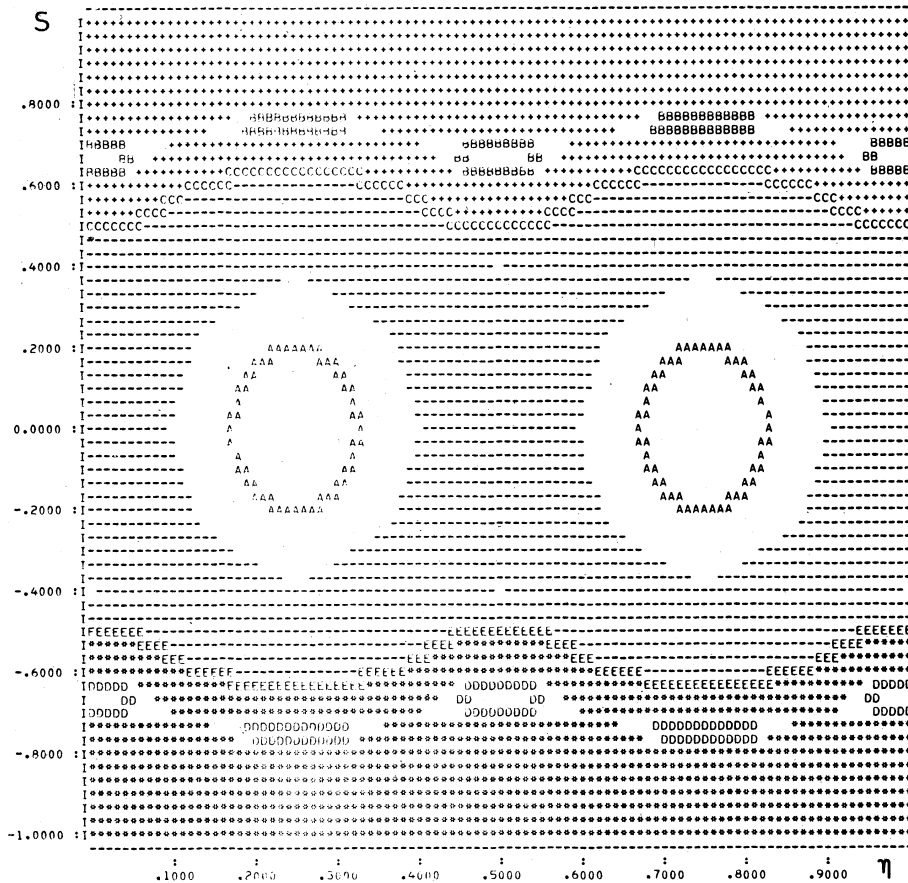


FIG. 10. Graphical analysis of ϕ for $\delta = 0.76$, showing the first observed subdivision in stochastic components.

divides into invariant parts, correspondingly λ_{\max} undergoes a bifurcation. The whole situation is illustrated in the branched graph of Fig. 13; vertical bars, as in Fig. 4, represent the uncertainty by which λ_{\max} has been determined. Notice that they are small for small δ , but appreciably larger for $\delta \geq 0.6$, where the stabilization time is considerably greater.

IV. ESTIMATE OF THE ENTROPY

A. Abramov formula and Piesin formula

In this section we give an estimate of the entropy of the billiard flow in the generalized stadium. We recall that if R is a transformation or a flow, which preserves the normalized measure μ , then $h_\mu(R)$ denotes the entropy of R with respect to measure μ . (See Refs. 7, 17, 18, and 25 for details.)

As in Ref. (12), for computing the entropy of our billiards we shall use Piesin's formula.¹⁹ However, at variance with respect to Ref. 12, this formula will not be applied directly to the billiard flow $\{T^t\}$, but to the transformation ϕ induced by the billiard flow on the global section N . Then, by the

Abramov formula (see Ref. 20 and Sec. 15 of Ref. 18), we shall finally obtain $h_{\mu_L}(\{T^t\})$.

Consider the general case of a billiard in a convex region Q of area $|Q|$, with differentiable border Γ . In $M = Q \times S^1$, besides the already employed system of coordinates (q_1, q_2, θ) , let us introduce new coordinates (τ, η, s) , where τ is the time run after the last collision and (η, s) are the coordinates of this collision (see Sec. IIIA).

It is easy to see that the determinant of the Jacobian $\partial(q_1, q_2, \theta)/\partial(\tau, \eta, s)$ is constant and equal to $|\Gamma|$. Consider now a point $x = (\eta, s) \in N$, with $s \neq \pm 1$, and denote by $l(x)$ the "time of first return" of x , i.e., the smallest $t > 0$ such that $T^t x \in N$. From the Abramov formula one obtains immediately

$$h_{\mu_L}(\{T^t\}) = \frac{h_{\nu_L}(\phi)}{\int_N l(x) d\nu_L} = \frac{2h_{\nu_L}(\phi)}{\int_N l(\eta, s) d\eta ds},$$

where ν_L , as in Sec. IIIA, denotes the normalized ϕ -invariant measure on N : $d\nu_L = \frac{1}{2} d\eta ds$.

But since

$$\det \frac{\partial(q_1, q_2, \theta)}{\partial(\tau, \eta, s)} = |\Gamma|,$$

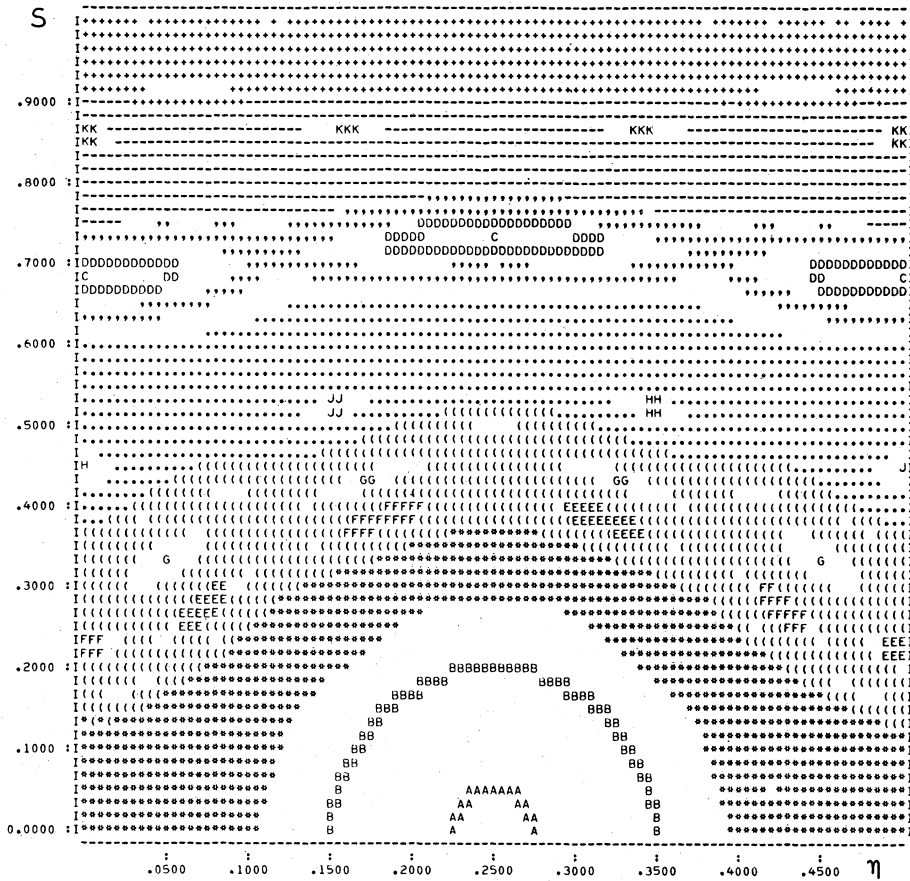


FIG. 11. Graphical analysis of ϕ for $\delta=0.85$ (enlargement of a quarter of the figure).

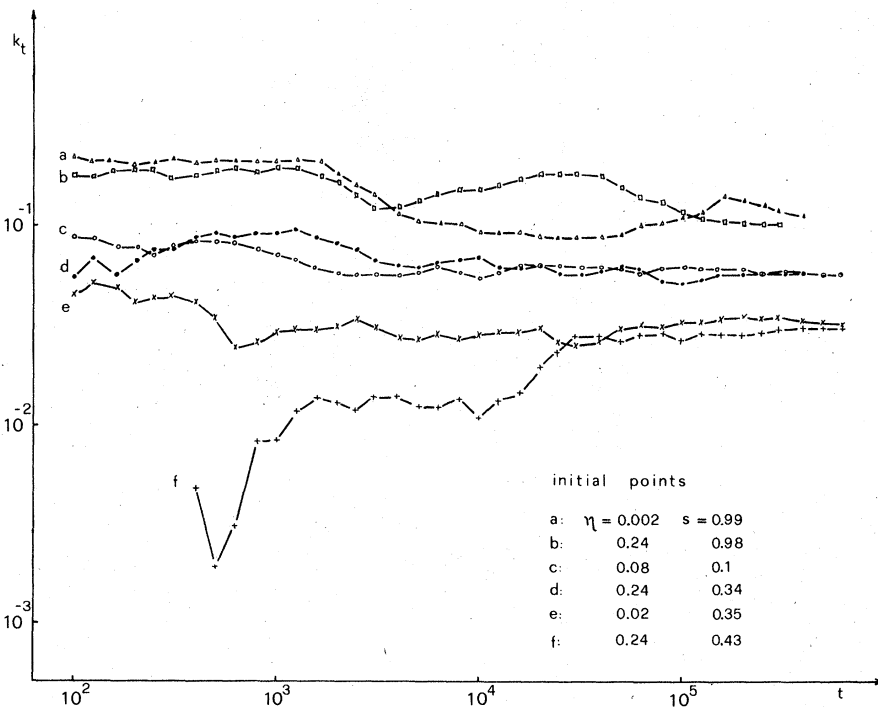


FIG. 12. Behavior of k_t for $\delta=0.85$ and initial points chosen in three different stochastic components.

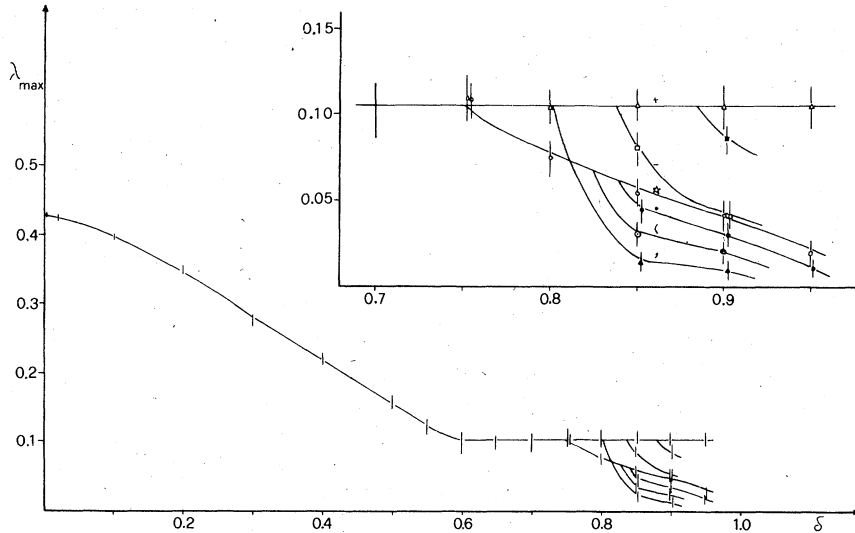


FIG. 13. Behavior of λ_{\max} as a function of δ . The different branches for $\delta \geq 0.76$ refer to the different stochastic components. An enlargement of the region where these branches appear is inserted; symbols +, -, etc. in it make the correspondence with the different stochastic components, as appearing in Fig. 11.

one has

$$\int_N l(\eta, s) d\eta ds = \int_M d\tau d\eta ds = \frac{1}{|\Gamma|} \int_M dq_1 dq_2 d\theta = \frac{2\pi |Q|}{|\Gamma|},$$

so that one finally obtains the equality

$$h_{\nu_L}(\{T^t\}) = \frac{|\Gamma|}{\pi |Q|} h_{\nu_L}(\phi),$$

which is at the basis of our computation.

Now, for determining $h_{\nu_L}(\phi)$ we will make use of Piesin's formula.¹⁹ Properly speaking, this formula has been proven in the hypothesis that ϕ is of class C^2 ; this requires that Γ is of class C^3 , while in our case Γ is only of class C^1 . Notice, however, that in the spirit of a numerical computation, the question of the differentiability of Γ in the four points P_1, \dots, P_4 is not very meaningful, as one can always imagine that suitable regularization in a small neighborhood of these points has been made. We thus suppose that Piesin's formula works well also in our case.

Piesin's formula says that

$$h_{\nu_L}(\phi) = \int_N \left(\sum_{\lambda_i^\phi(x) > 0} \lambda_i^\phi(x) \right) d\nu_L,$$

where $\lambda_1^\phi(x)$ and $\lambda_2^\phi(x)$ denote the LCN's of ϕ at the point x . Their definition is perfectly analogous to that given in Sec. II B for the flow $\{T^t\}$; one has simply to replace the time t by the number of iterations of the mapping. Their properties are also analogous, but, since N is of dimension two, at most two distinct values are present.

We shall suppose $\lambda_1^\phi(x) \geq \lambda_2^\phi(x)$; $\lambda_1^\phi(x)$ will be denoted also by $\lambda_{\max}^\phi(x)$. The numerical technique for computing $\lambda_{\max}^\phi(x)$ is very similar to that described in Sec. II B: Given a point $x \in N$, and a sufficiently small segment f with ends in x and $y \in N$, one computes the parameter $k_n(x, \vec{f})$, expecting that for a random choice of \vec{f} it approaches the limit value $\lambda_{\max}^\phi(x)$. Concerning the norm, we notice that in the tangent spaces to N we used the same norm $\|\cdot\|$ as in the computation of $k_i(x, \vec{e})$ in Secs. II and III.

It is easy to prove that one has $\lambda_2^\phi(x) = -\lambda_1^\phi(x)$, ν_L almost everywhere. Indeed, by applying to our case theorem 1 of Ref. 10, one finds that for ν_L almost everywhere it is

$$\lambda_1^\phi(x) + \lambda_2^\phi(x) = \lim_{n \rightarrow \infty} (1/n) \ln |\det d\phi_x^n|,$$

where $\det d\phi_x^n$ denotes the determinant of the Jacobian matrix of the application ϕ^n at point x , computed in the coordinates (ψ, α) . Let $\rho(x) = \cos \alpha$, for $x = (\psi, \alpha) \in N$. As the measure $\cos \alpha d\psi d\alpha$ is ϕ invariant, one has $|\det d\phi_x| = \rho(x)/\rho(\phi x)$ and consequently,

$$|\det d\phi_x^n| = \prod_{k=1}^n \frac{\rho(\phi^{k-1}x)}{\rho(\phi^k x)}.$$

Applying now the Birkhoff ergodic theorem to the function $\ln[\rho(x)]$ [it is easy to see that $\ln[\rho(x)] \in L^1(N, \nu_L)$] one obtains that for ν_L almost everywhere one has

$$\begin{aligned} \lim_{n \rightarrow \infty} \frac{1}{n} \ln |\det d\phi_x^n| &= \lim_{n \rightarrow \infty} \frac{1}{n} \sum_{k=1}^n \ln[\rho(\phi^{k-1}x)] \\ &\quad - \lim_{n \rightarrow \infty} \frac{1}{n} \sum_{k=1}^n \ln[\rho(\phi^k x)] = 0. \end{aligned}$$

We have thus $\lambda_2^\phi(x) = -\lambda_1^\phi(x)$,²⁸ so that in our case

Piesin's formula reduces to the equality

$$h_{\nu_L}(\phi) = \int_N \lambda_{\max}^\phi(x) d\nu_L(x).$$

B. Numerical estimate of the entropy

Now, to apply Piesin's formula for computing $h_{\nu_L}(\phi)$, we shall use the assumption that $\lambda_{\max}^\phi(x)$ is ν_L almost everywhere constant, within each stochastic component of ϕ . This is not proven, but the numerical evidence is strong: in any case, for initial points in the same components, we found the same λ_{\max}^ϕ (the same happens also for λ_{\max} of the flow $\{T^t\}$). With this assumption one obtains that the integral in Piesin's formula reduces trivially to a sum, and one has

$$h_{\nu_L}(\phi) = \sum_i \nu_L(S_i) \lambda_{1,i}^\phi,$$

where S_1, S_2, \dots denote the stochastic components of ϕ and $\lambda_{1,i}^\phi$ denotes the maximal LCN in S_i . A rough estimate of $\nu_L(S_i)$ can be performed directly on the figures. A practical method is that of (automatically!) counting the number of symbols in each picture. In this way one obtains an estimate of $h_{\nu_L}(\phi)$, and consequently of $h_{\nu_L}(\{T^t\})$, for any value of δ ; the result for the latter is reported in Fig. 14. Notice that, at variance with the measurements of λ_{\max} (Figs. 4 and 13), here it is not possible to give an estimate of the errors, because the uncertainty in the measurements of $\nu_L(S_i)$ is not known (probably the measures are over-estimated, since microscopic islands are not visible in our rough pictures). Figure 14 gives a weak indication that $h_{\nu_L}(\{T^t\})$ is not a monotonically decreasing function of δ . Certainly, this may be an illusion produced by the errors. Notice however that the arc of positive slope occurs just before the first observed separation of the stochastic region into invariant components.

V. CONCLUDING REMARKS

Our numerical experiments show that the stochastic transition can take place for systems of

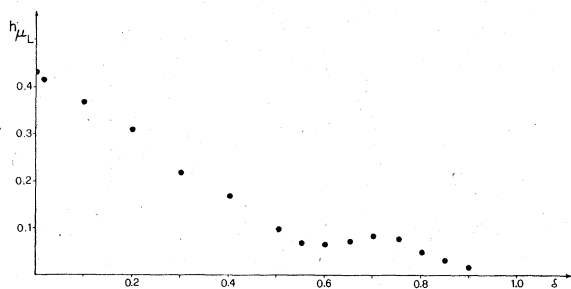


FIG. 14. Estimate of the entropy at different values of δ .

very simple geometrical nature. Billiards seem to us to be rather interesting systems from the point of view of numerical investigations: Indeed they are sufficiently simple to be easily handled with a computer, but nevertheless physically significant, and several theoretical investigations on them are presently available. Of course the final goal would be that of proving theoretically the existence of the numerically observed phenomena.

Concerning the existence of separated stochastic components, we remark that numerical evidence of this fact has been obtained recently by Carotta *et al.*²⁷ for a completely different model, namely, a chain of particles interacting via a Lennard-Jones potential. We believe that the existence of several distinct stochastic components in the intermediate stages of a stochastic transition is not an exceptional phenomenon, but probably a very frequent one. Unfortunately, it is not so easy to put it in evidence by numerical methods in all interesting situations.

ACKNOWLEDGMENTS

We are very grateful to Dr. A. B. Katok (Moscow) for communicating to us several results concerning billiards, and to Dr. J. G. Sinai (Moscow) for some important remarks and suggestions. We are also indebted to Dr. L. Galgani (Milano) and to Dr. S. Wojciechowski (Warsaw) for helpful discussions and for reviewing the manuscript.

APPENDIX: SOME MATHEMATICAL COMMENTS

As already remarked in the Introduction, the ergodic properties of a billiard in the generalized stadium for $0 < \delta < 1$ are not known theoretically. Features like coexistence of an ordered and a stochastic region, separation of the latter into invariant components, and positivity of entropy for $0 < \delta < 1$ are only numerical results. Nevertheless, in light of some theoretical results of Lazutkin²¹ and of Dvorin and Lazutkin,²² it is possible to draw a heuristical picture that partially explains the numerically observed features. These theoretical results refer to billiards in strictly convex regions with sufficiently differentiable border, so that they are not directly applicable to our billiards. However, as remarked in Sec. IV A, the question of differentiability in P_1, \dots, P_4 is not very meaningful from the point of view of numerical computations, and it is natural to suppose that this is not the essential point.

Let us give a short summary of these results. Consider a strictly convex, compact region Q of the plane R^2 with differentiable border Γ . A closed convex differentiable curve $L \subset Q$, $L \neq \Gamma$, is called a caustic in Q if any trajectory of the billiard in

Q , which once is tangent to L , is again tangent to L after each reflection. For example, the caustics in a disk are all the circles concentric with the disk. Clearly, if L is a caustic in Q , then each trajectory traversing once the region limited by L traverses again such region after each reflection; it easily follows that the presence of one caustic in Q is sufficient to ensure that the billiard in Q is not ergodic with respect to the Liouville measure.

In general, the existence of caustics is not evident. In Ref. 21 it is proved that if Γ is sufficiently differentiable, then in any neighborhood of Γ in Q , infinitely many caustics exist whose union is a set of positive, plane Lebesgue measure.

Suppose now that a given stochastic trajectory (i.e., a trajectory with positive λ_{\max}) undergoes a collision (η, s) with the border, with $|s|$ sufficiently close to 1. Such a trajectory certainly traverses the annulus between two caustics, crossing the more external one but not the more internal. The same clearly happens after each reflection, so that the trajectory is in a sense "confined" to the annulus.

This picture seems to be rather appropriate for heuristically interpreting the numerical results of Sec. III B. Indeed, it is evident that all orbits tangent to a given caustic give rise to traces, in the section N of the flow, belonging to a curve $s = s(\eta)$, while orbits confined (in the above sense) to an annulus limited by two caustics L_1 and L_2 produce traces in N which are confined in the strip

between two curves $s_1(\eta)$ and $s_2(\eta)$. The separation of the sea into an increasing number of invariant components when $\delta \rightarrow 1$ is then interpreted as the appearance of an increasing number of caustics (of course, only the caustics which are sufficiently apart from Γ give rise to macroscopically observable stochastic components).

Concerning now the stochastic properties of our billiards, let us make a final remark. It is well known that the very strong stochastic properties of Anosov systems and certain related systems²³⁻²⁵ are accompanied by a relevant feature, i.e., that such systems admit of infinitely many periodic orbits of hyperbolic type, with arbitrary large periods.^{23,25}

Now, it is proved in Ref. 22 that for a residual set (in the sense of Baire category²⁶) of billiards in compact strictly convex regions, with border of class C^r , $8 \leq r \leq \infty$, the diffeomorphism ϕ has the above property. It is then not so surprising that in the case of the generalized stadium, stochasticity is numerically observed even for δ not too small. In our knowledge, no other property of billiards in strictly convex regions, concerning the stochastic properties, has been proved.

Note added in proof. The complete demonstration of Piesin's formula has been now published [Ya. B. Piesin, *Usp. Mat. Nauk.* **32**, 55 (1977)]. Another demonstration has been announced by V. M. Milionščikov [Differentialnyje Uravnemja **12**, 2188 (1976)].

¹E. Fermi, J. Pasta, and S. Ulam, Los Alamos Scientific Lab. Report No. LA-1940 (1955) [E. Fermi, *Collected Papers* (University of Chicago, Chicago, 1965); S. Ulam, *Sets, Numbers and Universes* (MIT, Cambridge, Mass., 1974)].

²J. Ford, in *Fundamental Problems in Statistical Mechanics*, edited by E. D. G. Cohen (North-Holland, Amsterdam, 1975), Vol. 3.

³B. V. Chirikov, Researches concerning the theory of nonlinear resonances and stochasticity. CERN Trans. No. 71-40, Geneva, 1971 (unpublished).

⁴B. V. Chirikov and F. M. Izrailev, in *Colloque International CNRS sur les Transformations Ponctuelles et leurs Applications* (Edition du CNRS, Paris, 1976).

⁵M. Hénon and C. Heiles, *Astron. J.* **69**, 73 (1964).

⁶For the definition of completely integrable systems, K flows, and entropy, see, for example, Ref. 7, where the completely integrable systems are called integrable. For more information concerning ergodic theory and, in particular, entropy, see Refs. 17, 18, and 25.

⁷V. I. Arnold, A. Avez, *Problèmes Ergodiques de la Mécanique Classique* (Gauthier Villars, Paris, 1967) [English edition: *Ergodic Problems of Classical Me-*

chanics (Benjamin, New York, 1968)].

⁸L. A. Bunimovich, *Funkt. Analiz. Jogo Prilog.* **8**, 73 (1974) [*Funct. Anal. Appl.* **8**, 254 (1974)].

⁹V. F. Lazutkin, *Izv. Akad. Nauk. SSSR Ser. Mat.* **37**, 437 (1973) [*Math. USSR-Izv.* **7**, 439 (1973)] asserts that coexistence of invariant tori and a stochastic region has to be present for billiards in strictly convex regions. However, neither a theoretical proof nor a numerical evidence are produced.

¹⁰V. I. Oseledec, *Tr. Mosk. Mat. Obsch.* **19**, 179 (1968) [*Trans. Mosc. Math. Soc.* **19**, 197 (1968)].

¹¹M. Casartelli, E. Diana, L. Galgani, and A. Scotti, *Phys. Rev. A* **13**, 1921 (1976).

¹²G. Benettin, L. Galgani, and J.-M. Strelccyn, *Phys. Rev. A* **14**, 2338 (1976).

¹³G. D. Birkhoff, *Dynamical Systems* (American Mathematics Society, Providence, R.I., 1927).

¹⁴G. Gallavotti, in *Dynamical Systems, Theory and Applications. Lecture Notes in Physics* (Springer-Verlag, Berlin, 1975), Vol. 38.

¹⁵Properly speaking, for some of the points $x = (q, v) \in M$, with $q \in \Gamma$, the flow $\{T^t\}$ is not defined, but we can disregard these points since they constitute a set of zero

- μ_L measure.
- ¹⁶For the notion of global section, see for example, Z. Nitecki, *Differentiable Dynamics* (MIT, Cambridge, Mass., 1971). The global section is here simply called the section.
- ¹⁷Ya. G. Sinai, *Theory of Dynamical Systems*, part I of Lect. Notes Ser. Math. Inst. Aarhus Univ. No. 23 (1970) (unpublished).
- ¹⁸Ya. G. Sinai, *Introduction to Ergodic Theory. Mathematics Notes* (Princeton University, Princeton, N.J., 1976), Vol. 18.
- ¹⁹Ya. B. Piesin, Dokl. Akad. Nauk. SSSR 226, 774 (1976) [Soviet Math. Dokl. 17, 196 (1976)].
- ²⁰L. M. Abramov, Dokl. Akad. Nauk. SSSR 128, 873 (1959) [English translation in Amer. Math. Soc. Trans. 49, 167 (1966)].
- ²¹V. F. Lazutkin, Izv. Akad. Nauk. SSSR Ser. Mat. 37, 186 (1973) [Math. USSR-Izv. 7, 185 (1973)].
- ²²M. M. Dvorin and V. F. Lazutkin, Funkt. Anal. Jogo Prilog. 7, 20 (1973) [Funct. Anal. Appl. 7, 103 (1974)].
- ²³D. V. Anosov, Trudy Math. Inst. Steklov No. 90 (Akad. Nauk. SSSR, Moscow, 1967) [Proc. Steklov Inst. Math. No. 90 (American Mathematical Society, Providence, R.I., 1969)].
- ²⁴S. Smale, Bull. Am. Math. Soc. 73, 747 (1967).
- ²⁵R. Bowen, *Equilibrium States and the Ergodic Theory of Anosov Diffeomorphisms, Lectures Notes in Mathematics* (Springer-Verlag, Berlin, 1975), Vol. 470.
- ²⁶N. Dunford and J. T. Schwartz, *Linear Operators* (Interscience, New York, 1958), Part I.
- ²⁷M. C. Carotta, C. Ferrario, G. Lo Vecchio, and L. Galgani, Phys. Rev. A 17, 786 (1978).
- ²⁸In a similar way one can easily prove that (in the notation of Ref. 12) for $N=2$ and fixed E , one has $\lambda_1(x) = -\lambda_{-1}(x)\mu_L$ - almost everywhere on Γ_E . The "experimental" test of this equality in Ref. 12 is then unnecessary.